

The Influence of Ice Cover on Two Lake-Effect Snow Events over Lake Erie

JASON M. CORDEIRA

Department of Earth and Atmospheric Sciences, University at Albany, State University of New York, Albany, New York

NEIL F. LAIRD

Department of Geoscience, Hobart and William Smith Colleges, Geneva, New York

(Manuscript received 17 July 2007, in final form 15 November 2007)

ABSTRACT

It is generally understood that extensive regions of significant lake ice cover impact lake-effect (LE) snow storms by decreasing the upward heat and moisture fluxes from the lake surface; however, it is only recently that studies have been conducted to more thoroughly examine this relationship. This study provides the first examination of Great Lakes LE snow storms that developed in association with an extensively ice-covered lake. The LE snow events that occurred downwind of Lake Erie on 12–14 February 2003 and 28–31 January 2004 produced maximum snowfall totals of 43 and 64 cm in western New York state, respectively. The presence of widespread ice cover led these snows to be less anticipated than snowfalls from Lake Ontario, which had limited ice cover. For both events, a variety of ice-cover conditions and meso- and synoptic-scale factors (i) helped support LE snow storm development, (ii) lead to the transitions in LE convective type, and (iii) resulted in noteworthy snowfalls near Lake Erie. Thinner ice cover along with favorable fetch directions during the 2004 event likely aided the development of more significant snowband time periods and the resulting greater snowfall. Although Lake Erie had regions with lower ice concentration during the 2003 event, thicker ice cover was present across a greater area of the lake, fetch directions during lake-effect time periods were positioned over higher ice concentration regions, and snowbands had a shorter duration and impacted the same region to a lesser degree than the 2004 case.

1. Introduction

Temporal and spatial variations of ice cover are known to affect lake-effect (LE) systems by limiting surface heat and moisture exchanges (Niziol et al. 1995) and altering mesoscale circulation development, evolution, and morphology (Laird and Kristovich 2004). The presence of widespread ice cover over regions of the Great Lakes coupled with the limited understanding regarding the development of LE storms over ice-covered lakes often provides significant challenges to winter weather forecasting (Thomas Niziol, Buffalo, and Daniel Leins, Cleveland National Weather Service Forecast Offices 2006, personal communications). Great Lakes ice cover is often very transitory during the winter, particularly in midlake and upwind shore-

line areas where changes in temperature, wind speed, and wind direction can cause a shift, compaction, dissipation, or expansion of the ice field (e.g., Richards 1964). Although a continuous-unbroken ice cover rarely forms on most of the Great Lakes, extensive regions of high ice concentration (amount of ice cover per unit area of lake) often develop. Ice usually begins to form on the Great Lakes in December and January and reaches the maximum spatial coverage in February or early March (Assel 1990, 1999); however, observations for Lake Erie, the shallowest of the Great Lakes, show that >90% of the lake is commonly ice covered by early January (Assel et al. 2002).

Despite the noted importance of ice cover to winter weather forecasting in the Great Lakes region (Niziol et al. 1995; Rauber and Ralph 2004), the influence of variable ice concentrations on LE boundary layers and mesoscale systems has only recently begun to be investigated. Laird and Kristovich (2004) examined historical Great Lakes LE events and found 11 events when cloud bands developed during periods of extensive lake

Corresponding author address: Neil F. Laird, Department of Geoscience, Hobart and William Smith Colleges, 4002 Scandling Center, Geneva, NY 14456.
E-mail: laird@hws.edu

ice coverage; 8 events occurred when the underlying lake had $\geq 80\%$ ice concentration and 3 events occurred when ice concentration was $\geq 95\%$ over the entire lake. Additionally, Gerbush et al. (2008) used aircraft measurements from over Lake Erie during the Great Lakes Ice Cover–Atmospheric Flux (GLICAF) project to determine that estimated surface sensible heat fluxes increased rapidly to open-water values as the ice concentration decreased from 100% to about 70%.

Ice thickness can also have an important influence on surface sensible and latent heat fluxes. Although environmental conditions are often distinctly different between winter events in the Great Lakes and Arctic regions, a numerical study of Arctic leads by Zulauf and Krueger (2003) found that significant surface fluxes can continue to occur over ice-covered leads. Their numerical simulations showed that surface sensible (latent) heat fluxes over a frozen lead are 81% (47%) of the value for an unfrozen lead. Additionally, their simulations approximated a 50% (25%) decrease in sensible heat flux as ice thickness increased from 0 to 10 cm (10 to 20 cm). The authors are not aware of any studies that have investigated the impact of ice thickness on surface heat fluxes for the Great Lakes.

Past investigations of LE snow storms in the Great Lakes region have primarily focused on events that have developed over ice-free regions (e.g., Braham 1983; Reinking et al. 1993; Ballentine et al. 1998; Kristovich et al. 2000). This study presents two LE snow events that occurred downwind of Lake Erie on 12–14 February 2003 and 28–31 January 2004, which lead to maximum snowfall totals of 43 and 64 cm, respectively, in western New York state during time periods when widespread ice cover was present over Lake Erie (Fig. 1). In both cases, the presence of widespread ice cover led the Lake Erie snows to be less anticipated than significant snowfalls from Lake Ontario, which had limited ice cover. The purpose of this investigation is to examine the influence that spatially extensive and variable Lake Erie ice cover had on the development and evolution of the LE snow storms.

The data and information used to examine the February 2003 and January 2004 cases are provided in section 2. The synoptic conditions, mesoscale evolution, and ice cover attributes for the 2003 and 2004 cases are presented in sections 3 and 4, respectively. Section 5 provides a discussion of the influence of spatially varied distributions of ice concentration and thickness along with a summary of the investigation.

2. Data and methods

This observational study incorporates a variety of datasets (i.e., surface, radar, sounding, and satellite)

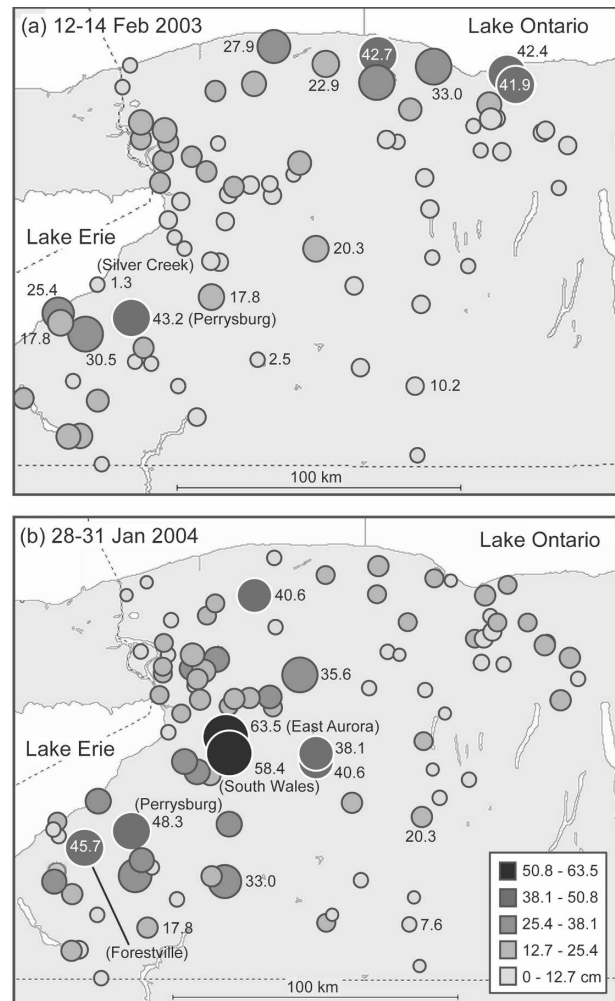


FIG. 1. Lake-effect snowfall totals (cm) downwind of Lake Erie for (a) 12–14 Feb 2003 and (b) 28–31 Jan 2004. (Snowfall data was made available courtesy of NWS Buffalo.)

from two cases to better understand the influence of Lake Erie ice cover on the development and evolution of LE snow storms. Snow spotter reports archived by the National Weather Service (NWS) at Buffalo, New York, provided snowfall data. Snowfall totals from each of the events are shown in Fig. 1 and demonstrate the localized spatial distribution of LE snowfall in western New York, east of Lake Erie. For each event, larger snowfall amounts occurred within approximately 50 km of the southeastern shore of Lake Erie. Snowfall amounts >40 cm also occurred near the southeastern shore of Lake Ontario during the 2003 case in association with LE snowbands originating from the ice-free open waters of Lake Ontario.

Surface and 850-hPa weather charts produced by the National Centers for Environmental Prediction (NCEP) and obtained from the National Climatic Data

Center (NCDC) were examined to assess the temporal evolution of the synoptic-scale influences on both events. Temperature, dewpoint temperature, and wind speed and direction information from surface stations along the shoreline of Lake Erie and lake temperature information from the Great Lakes Environmental Research Laboratory (GLERL) Great Lakes Surface Environmental Analysis (GLSEA) were used to characterize the mesoscale environment and estimate heat and moisture fluxes with bulk transfer methods (Kristovich and Laird 1998; Garratt 1992). The regional atmospheric conditions were represented using a lake-area average of measurements from nine surface stations in close proximity to Lake Erie. The surface stations included four sites located upwind or north [Erieau, Ontario, Canada (CWAJ); London, Ontario, Canada (CYXU); Port Huron St. Clair Airport (KPHN); and Detroit Metro Airport (KDTW)] and five sites located downwind or south [Greater Buffalo International Airport, Buffalo, New York (KBUF); Chautauqua County/Dunkirk Airport, Dunkirk, New York (KDKK); Erie International Airport (KERI); Chautauqua County Airport, Jamestown, New York (KJHW); and Niagara Falls International Airport, Niagara Falls, New York (KIAG)] of the lake (Fig. 2a). Open-water fluxes were determined using a water temperature of 0°C for Lake Erie during both events because of the significant ice concentrations and the lack of available water temperature measurements for the Great Lakes during the winter season.

The Moderate Resolution Imaging Spectroradiometer (MODIS) and Geostationary Operational Environmental Satellite (GOES) imagery and Great Lakes ice charts from the National Ice Center (NIC) and the Canadian Ice Service provided ice distribution, concentration, and thickness information. Ice charts produced on a weekly basis were used to determine locations and areas of differing ice concentrations over Lake Erie. Figure 2 shows the ice concentration charts for Lake Erie prior to and during the 2003 and 2004 LE events. Ice thickness information available from the NIC is shown in Fig. 3 and represents the weekly chart closest in time to the dates of the events.

NIC ice analyses are produced by manual interpretation of data sources that include observations from ships, air reconnaissance, remote sensing data (i.e., visible, infrared, active, and passive microwave), and model output (Fetterer and Fowler 2006). A detailed quality assessment of NIC ice charts has not been completed; however, the manual form of multisensory data fusion and data assimilation produces ice information more accurate than using any single data source or an automated approach (Fetterer and Fowler 2006). Meta-

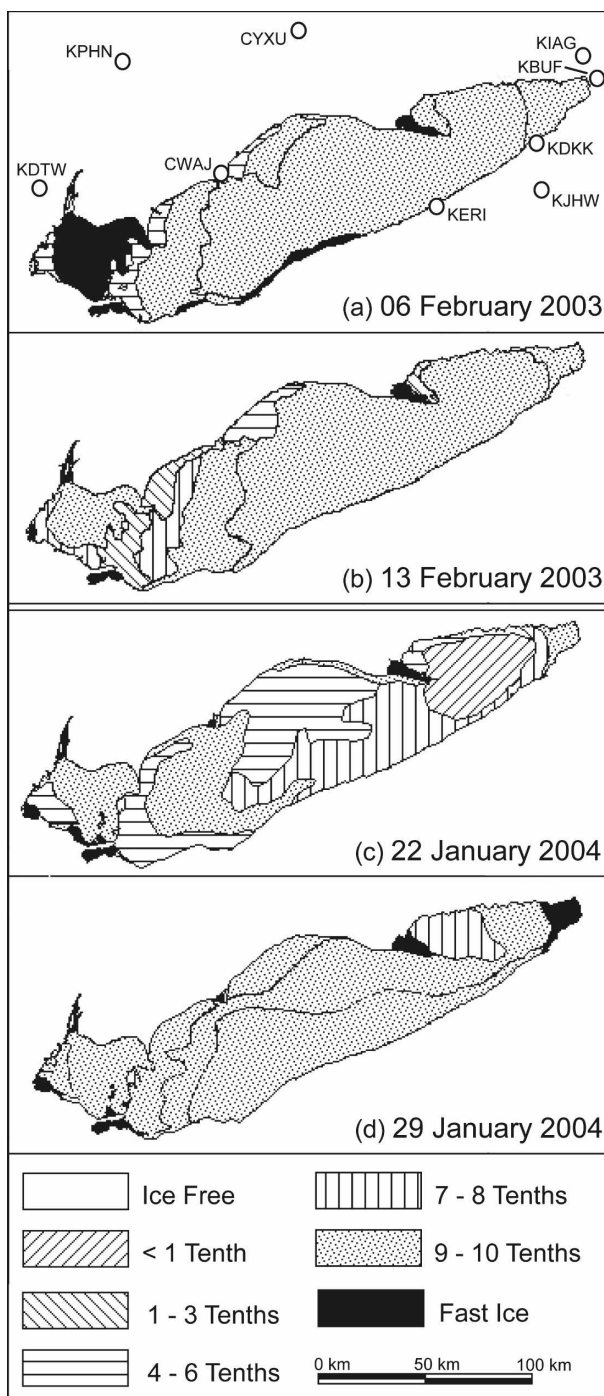


FIG. 2. Distribution of ice concentrations for Lake Erie for time periods prior to and during the (a),(b) 2003 and (c),(d) 2004 cases. Ice concentration is shown using hatched fill representing tenths of unit area covered by ice. Ice concentration data was made available from the NIC. Surface stations used to estimate lake-area average conditions are shown in (a).

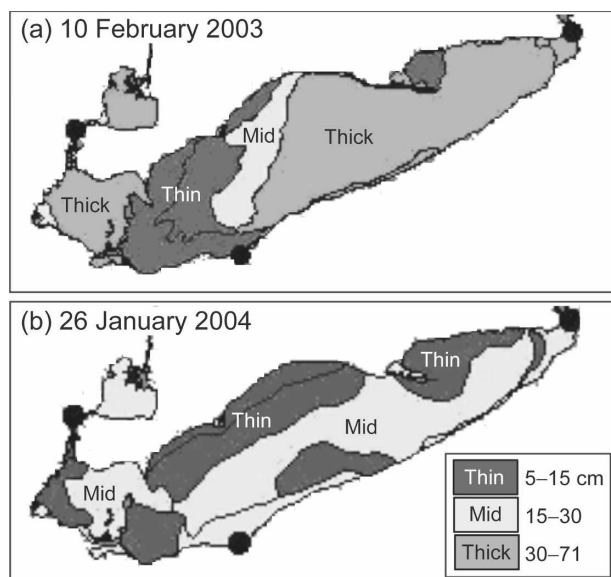


FIG. 3. Distribution of ice thicknesses for Lake Erie for the (a) 2003 and (b) 2004 cases. Data was made available from the NIC.

data associated with the ice analyses created during the 2003 and 2004 lake-effect events states that the Lake Erie area used RADARSAT satellite data for 2003 analysis (Fig. 2b) and a combination of RADARSAT and the Advanced Very High Resolution Radiometer (AVHRR) data was used for the 2004 ice analysis (Fig. 2d). Although potential error uncertainty has not been thoroughly investigated for the NIC ice analyses, Partington et al. (2003) cites $\pm 5\%$ – 10% as the accuracy of ice concentration estimates. This level of uncertainty seems to be consistent with differences between MODIS imagery and NIC ice concentrations that are presented in sections 3b and 4b.

For each of the cases a total energy transfer (TET) analysis was conducted to examine the role of Lake Erie on exchanging energy with and modifying the regional atmosphere. Total energy transfer is defined as the product of the water surface area (taking into account variable ice concentrations) and total heat flux (i.e., sensible and latent), similar to an approach used by Jeffries and Morris (2006) to estimate the total, lake-wide conductive heat loss for the Great Slave Lake. The TET provides information related to the thermodynamic processes controlling the modification of the lower-tropospheric stability in the vicinity of the lake; however, it should be noted that our estimate assumes no energy transfer through ice areas and thus provides an underestimate since conductive heat transfer is reduced, but still present in regions of complete ice cover (e.g., Maykut 1978; Lytle and Ackley 1996; Sturm et al. 2002; Zulauf and Krueger 2003; Jeffries and Morris 2006).

Level II Weather Surveillance Radar-1988 Doppler (WSR-88D) radar reflectivity data collected at individual sites and regional composite reflectivity fields were used to examine the distribution, intensity, duration, and convective types of LE snowfall for Lakes Erie and Ontario. Two types of lake-effect convective regimes were dominant during each case—shoreline snowbands (SBs) and widespread coverage—the latter consisting of both horizontal roll and cellular convection (HRC). In addition, transitions between SB and HRC were observed over and downwind of Lake Erie during the 2003 and 2004 events.

Dependent upon the ice-cover distribution and variation in wind directions, fetch distances over regions of open water can be significantly altered and result in differences in LE convective type (Laird and Kristovich 2004). An examination of the linkage between ice-cover concentration, ice thickness, overlake air parcel trajectories, and snowfall regions downwind of Lake Erie was supported with the use of the Hybrid Single-Particle Lagrangian Integrated Trajectory (HYSPPLIT) model (Draxler and Hess 1997; Draxler and Hess 1998; Draxler and Rolph 2003; Rolph 2003). The model was run for a 12-h time period for each trajectory simulation using the North American Mesoscale Eta Data Assimilation System (EDAS) archived datasets. Model back trajectories were conducted for several locations downwind of Lake Erie for identified time periods of differing LE convective type during each case. Back trajectories were initiated at a height of 100 m at a time representing the midpoint of each LE convective-type time period. The trajectory start locations were positioned at the center of the greatest snowfall regions, which were determined from WSR-88D radar and NWS snow spotter datasets.

3. Case 1: 12–14 February 2003

a. Regional conditions overview

At 1200 UTC 11 February 2003 a strong cold front had moved through the Northeast as a region of weak high pressure moved eastward across the eastern Great Lakes (Fig. 4a). Surface temperatures near Lakes Erie and Ontario were between -5.0° and -10.0°C with surface winds from the south at approximately 5 m s^{-1} . A strengthening Midwestern low pressure center crossed the eastern Great Lakes shortly before 1200 UTC 12 February (Fig. 4c). At 850 hPa, strong cold advection from central Canada brought cold air (-20°C) into the eastern Great Lakes region beginning during the period of 0000–1200 UTC 12 February (Fig. 4d).

Moderate-to-heavy synoptic-scale snowfall, accompanying the frontal passage on 12 February, departed

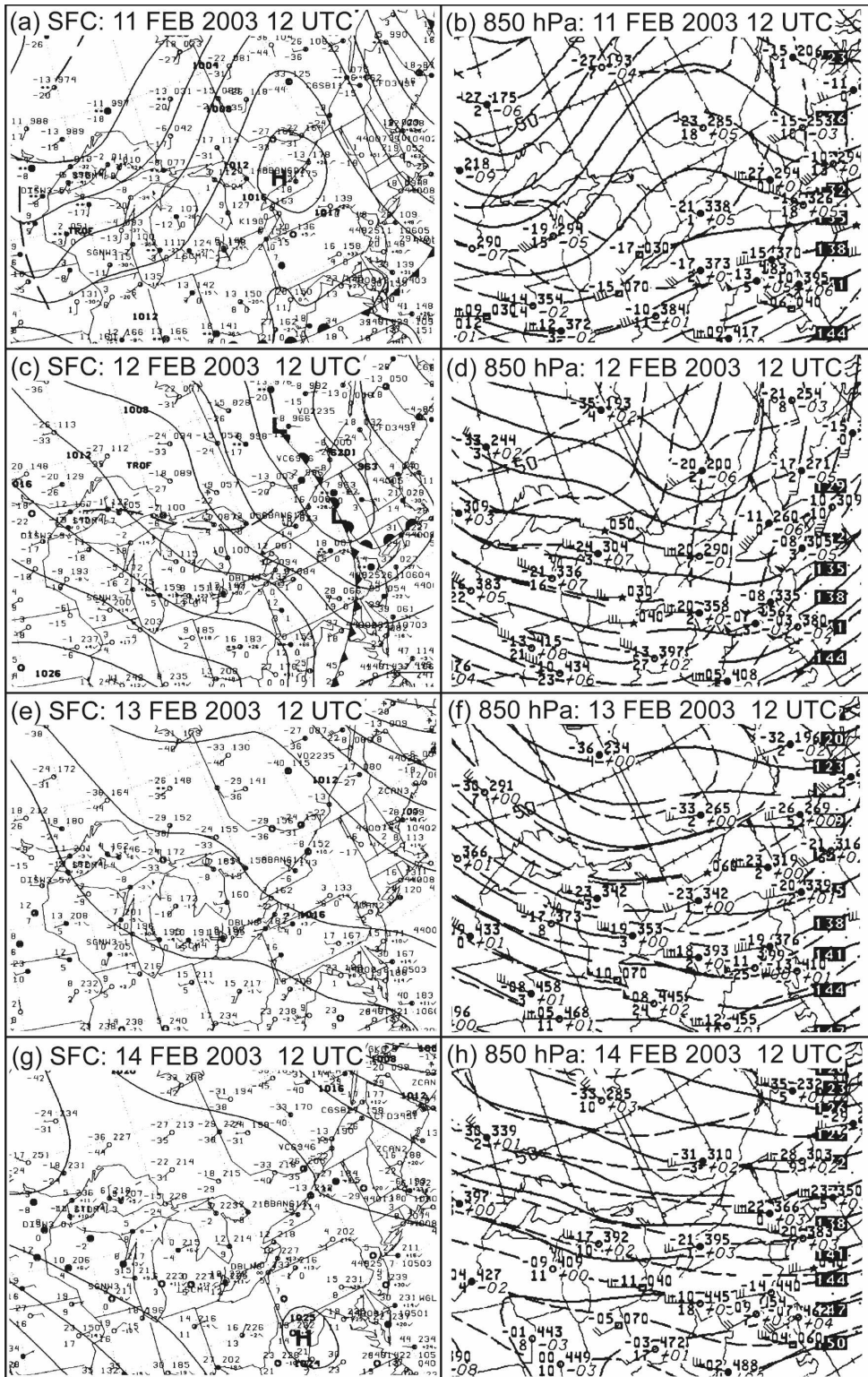


FIG. 4. Surface and 850-hPa analyses for 1200 UTC (a),(b) 11 Feb; (c),(d) 12 Feb; (e),(f) 13 Feb; and (g),(h) 14 Feb 2003. Temperatures on surface (850 hPa) analyses are provided using degrees Fahrenheit (Celsius). Analyses were made available from NCEP.

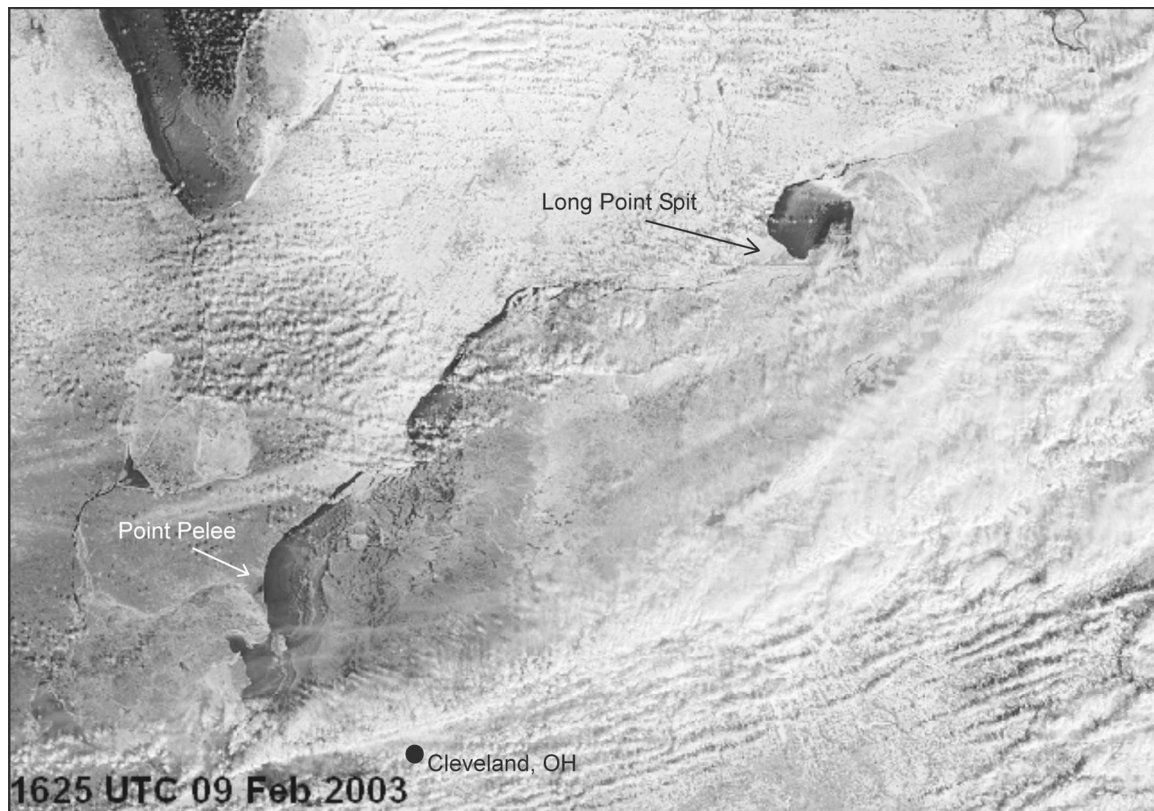


FIG. 5. MODIS satellite image of Lake Erie at 1625 UTC 9 Feb 2003, prior to lake-effect event. Darker areas represent low ice concentration or open-water regions. Image courtesy of MODIS Rapid Response Project at NASA GSFC.

the eastern Great Lakes region by 1200 UTC. Winds shifted to westerly behind the front and increased to 8 m s^{-1} , and surface temperatures dropped to between -10° and -15°C . The LE snowfall began on 12 February downwind of Lakes Erie and Ontario by 1200 and 1400 UTC, respectively. By 1200 UTC 12 February, the low-level (surface–850 hPa) lapse rates were approximately dry adiabatic ($-9.8^{\circ}\text{C km}^{-1}$) at KBUF. By 0000 UTC 13 February, a subsidence inversion developed above 750 hPa (not shown). Temperatures at 850 hPa decreased to -23°C over the eastern Great Lakes by 1200 UTC 13 February (Fig. 4f), and coupled with water temperatures of 0°C at the surface of Lake Erie, created significant convective potential.

By 1200 UTC 14 February, surface temperatures warmed to between -5.0° and -10.0°C and the surface pressure gradient reduced significantly causing winds to decrease to below 3 m s^{-1} (Fig. 4g). The LE snowfall dissipated near Lake Erie by 0700 UTC and light snowfall persisted over Lake Ontario until 2000 UTC.

b. Ice cover and energy transfer

Previous lake-effect studies have primarily focused on investigations and conditions when ice cover was not

present or not a contributing influence on mesoscale atmospheric systems. A detailed description and analysis of the Lake Erie ice cover is provided for the 2003 case in order to better understand the interaction between the lake-effect mesoscale systems and the underlying ice cover. The temporal evolution of the extensive ice cover over Lake Erie from 6 February to 13 February is shown in Figs. 2a,b. Leading up to the event, ice concentrations decreased in the western basin (from 4/10–6/10 to 1/10–3/10) and along the north central shoreline (from 9/10–10/10 to 4/10–6/10) and remained relatively constant at 9/10–10/10 over most of Lake Erie. The reduction in ice cover accounted for a 6% increase of Lake Erie open-water area; however, the regions were restricted to isolated areas with 1/10–7/10 ice concentration (Fig. 2b). MODIS satellite imagery at 1625 UTC 9 February showed areas of low ice concentration in the northwest portion of the eastern basin, east of the Long Point Spit, and in the western portion of the central basin, east of Point Pelee (Fig. 5). On 10 February, the NIC ice thickness chart showed thicknesses of 30–71 cm over most of the eastern basin and 5–15 cm in the central and western basins where ice concentrations were less than 8/10 (Figs. 3a and 2b).

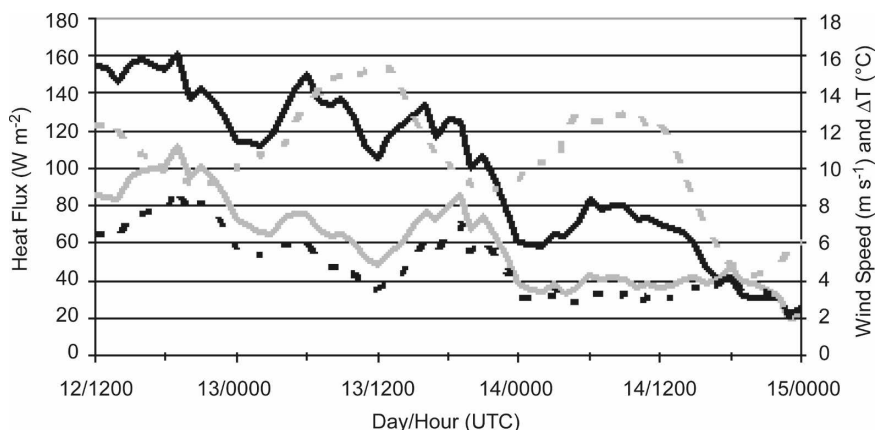


FIG. 6. Time series of lake-area-average sensible heat flux (black solid), latent heat flux (gray solid), wind speed (black dashed), and lake-air temperature difference (ΔT) (gray dashed) for Lake Erie during the 2003 event.

Open-water maximum total heat fluxes (combined sensible and latent) toward the beginning of the event (1200 UTC 12 February) were estimated to be nearly 250 W m^{-2} (Fig. 6). The total heat flux decreased during the event until reaching nearly 40 W m^{-2} at 0000 UTC 15 February. The lake-air temperature difference exhibited diurnal overnight maxima and daytime minima on 12 and 13 February; however, the temporal decrease in fluxes across the event was primarily a function of decreasing wind speed. The diurnal variation in lake-air temperature differences resulted from air temperature decreases overnight associated with radiational cooling. Kristovich and Spinar (2005) observed a similar diurnal pattern in lake-air temperature differences and surface heat fluxes and found them correlated with lake-effect precipitation occurrence near Lakes Superior and Michigan.

The lakewide TET (described in section 2) was significantly reduced over Lake Erie when taking into account the extensive distribution of ice cover. On 13 February, the TET for Lake Erie was 975 GW, a decrease of 85% from 6500 GW, the open-water TET under the same meteorological conditions. However, even with significant reductions in energy transfer from Lake Erie, the atmospheric environment favored the development of LE clouds and snowfall upward of 40 cm over localized regions of western New York.

c. Snowband evolution and mesoscale analysis

Lake-effect snowbands of varied location, intensity, duration, and convective type occurred in the vicinity of Lake Erie and led to the noteworthy snowfall. Snow totals in western New York, downwind of Lake Erie, ranged from about 1.3 cm at Silver Creek, New York, to 43 cm at Perrysburg, New York (Fig. 1a).

A time line of LE snow periods along with four representative analyses of the Lake Erie region are provided in Fig. 7 to assist in describing the linkage between lake-effect snowfall and variations in ice cover concentrations for Lake Erie. The SBs downwind of Lake Erie existed during four different time periods. The first three SB time periods, numbered 2, 4, and 5 on the Fig. 7 time line, affected a collocated region in southwestern New York. Similarly, two widespread coverage (HRC) time periods (numbered 1 and 3) affected the same area and aided in producing the larger localized snowfall totals (Fig. 1a). The fourth SB time period impacted an area north of Buffalo extending to the southwestern shore of Lake Ontario.

As the synoptic precipitation exited the eastern Great Lakes region, time periods with SB and HRC lake-effect organization initiated downwind of Lake Erie (Fig. 7). HRC downwind of Lake Erie developed south of Buffalo at 1200 UTC 12 February and covered a region to the Pennsylvania border (period 1 in Fig. 7). This region of HRC was positioned downwind relative to low ice concentration regions in the northern portions of the eastern and central lake basins; however, these low ice concentration areas were relatively small compared to the prevalent HRC observed in the radar reflectivity field and the individual lake-effect bands could not be directly associated with openings in the Lake Erie ice field. The HRC lasted until 0000 UTC 13 February when a shoreline band developed over the southern portion of Lake Erie with a westward extension to Lake Michigan. This band extended onshore east of Cleveland, Ohio, at 1900 UTC 12 February (period 1 in Fig. 7) and was associated with a region of warmer surface air temperatures (e.g., -7°C) and higher dewpoint temperatures over western Lake Erie.

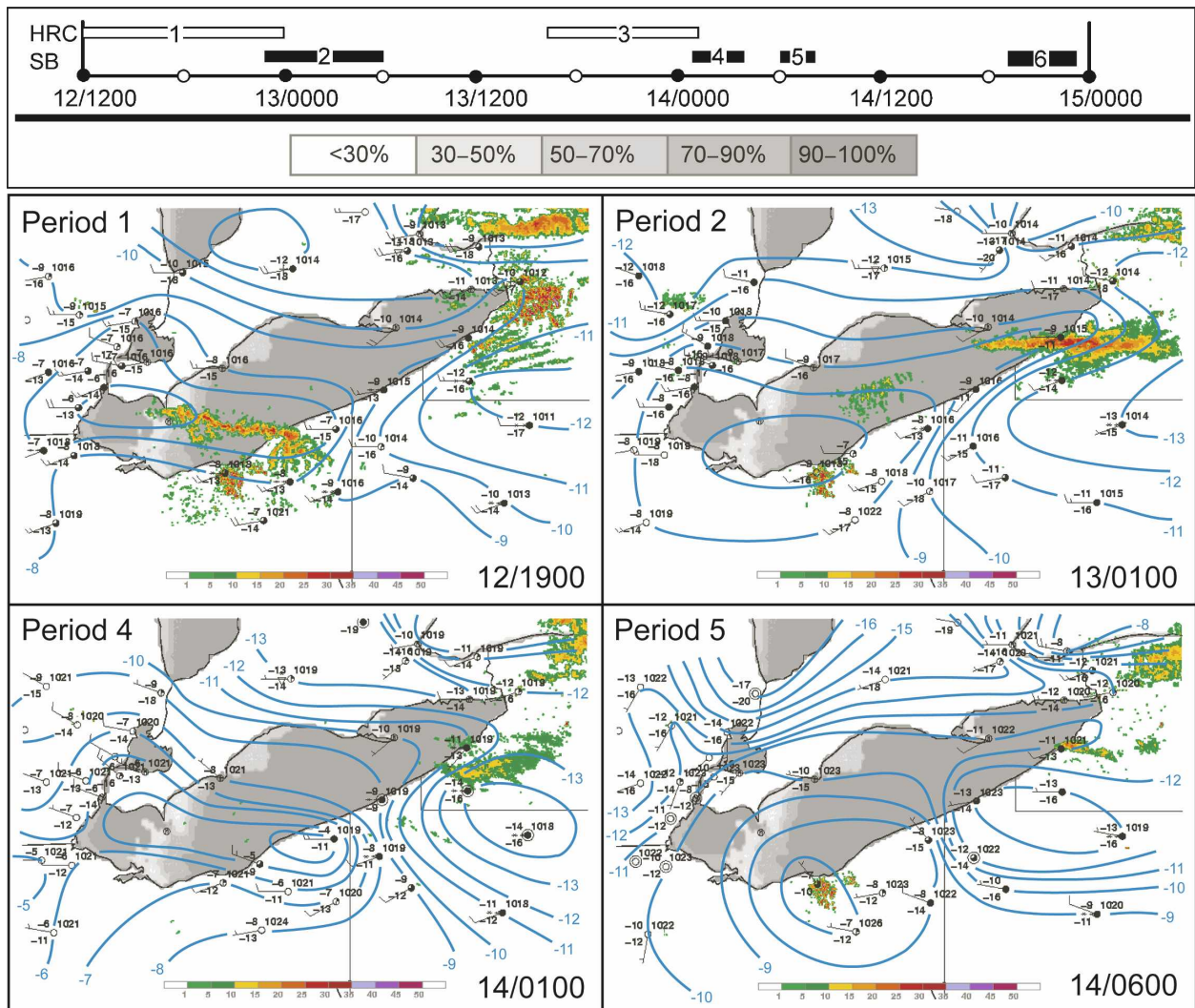


FIG. 7. Time line showing the temporal evolution of (a) lake-effect SBs and (b) widespread coverage (HRC) during 2003 event. Each time period is identified using consecutive number. Regional radar reflectivity (dBZ: color scale), surface station observations, ice concentration, and mesoscale temperature analysis are presented for several representative time periods. Isotherm analysis uses 1°C interval and the ice concentration scale (%) is shown below the time line.

By 2200 UTC 12 February, the shoreline band became the dominant precipitation band over southwestern New York (period 2 in Fig. 7) and remained positioned downwind of low ice concentration areas in the western basin as well as continuing to provide the linkage to Lake Michigan. The band moved onshore by 0300 UTC and dissipated by 0600 UTC as the band position shifted southward (i.e., inland).

HRC developed over southwestern New York at 1600 UTC 13 February and continued until 0100 UTC 14 February (period 3) when smaller-scale horizontal convective rolls merged into a single band over southwestern New York (period 4 in Fig. 7). Consolidation was brief as the shoreline band dissipated 3 h later

(0400 UTC 14 February) and was followed by a short-lived, isolated shoreline band on 14 February (period 5 in Fig. 7). Similarly, between 2000 and 2300 UTC an isolated, weak SB developed northeast of Buffalo (period 6). During these latter time periods, winds decreased in speed and had a greater southerly component (periods 4 and 5 in Fig. 7). The shift in wind conditions is clearly apparent in the meteogram from KDKK for the event (Fig. 8) and was also coordinated with a period of warming near the latter stages of the event (e.g., 1500 UTC 14 February).

Unlike shoreline bands 4, 5, and 6, the snowband that developed during time period 2 (i.e., 2300 UTC 12 February–0600 UTC 13 February) did not initiate over

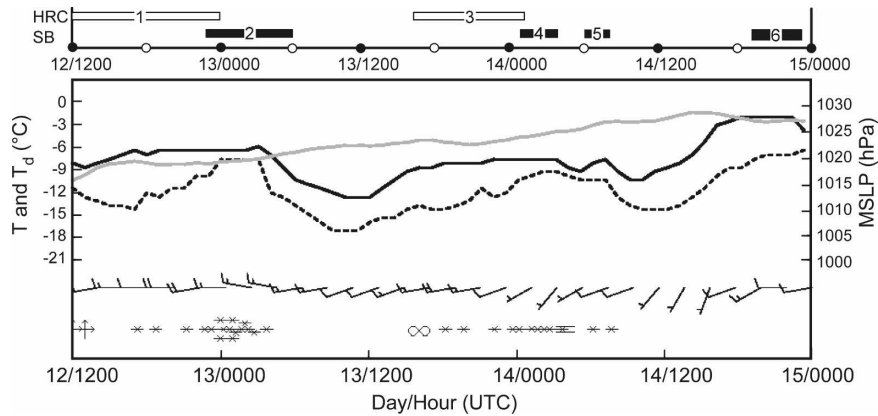


FIG. 8. Meteogram from KDKK for 2003 event showing temperature (T : black solid), dewpoint temperature (T_d : black dashed), MSLP (gray solid), wind barbs with speed and direction information, and weather conditions. The time line of HRC and SB lake-effect precipitation periods are also shown. Winds are represented as 2.55 and 5.1 m s^{-1} for short and long barbs, respectively. Report of weather conditions uses standard NWS symbols. The location of KDKK is shown in Fig. 2a.

Lake Erie. Both satellite and surface observations strongly suggest the band originated over Lake Michigan and maintained coherence as a moisture plume and low-level convergence zone across Lower Michigan until strengthening over the western basin of Lake Erie (periods 1 and 2 in Fig. 7). The temperature analyses for 1900 UTC 12 February and 0100 UTC 13 February (periods 1 and 2 in Fig. 7) show the modified air from Lake Michigan entering into the western Lake Erie region with an eastward extension along the southern shore of Lake Erie. This is most pronounced when the band is positioned directly over KDKK at 0100 UTC 13 February (period 2 in Fig. 7). This feature is similar to the lake-end pseudofront identified by Baker (1976) and lake-to-lake bands examined by Rose (2000) and Rodriguez et al. (2007). Although difficult to determine from analyses shown in Fig. 7, animations of radar reflectivity fields suggest this band intensified over the region of low ice concentrations in the western basin of Lake Erie before impacting areas of western New York. Maximum radar reflectivity values associated with this band from the Buffalo WSR-88D radar were nearly 35 dBZ for 4 h over southwestern New York.

4. Case 2: 28–31 January 2004

a. Regional conditions overview

At 0000 UTC 28 January 2004 a weak surface low pressure center present over southern Lake Huron was coupled with a positively tilted trough extending westward through northeastern Minnesota. The trough moved through the eastern Great Lakes by the after-

noon of 28 January (not shown). Synoptic precipitation crossed eastern Lake Erie by 1900 UTC with underlying HRC beginning on Lake Erie. The trough passage reinforced the region with colder air as winds shifted from southwest to west. Surface temperatures across western New York and Ontario, Canada, decreased from -6.0°C on 28 January to -10.0°C on 29 January (Figs. 9a–c). Concurrently, the region experienced cold-air advection as 850-hPa temperatures dropped from -15.0° to -20.0°C at Buffalo by 0000 UTC 30 January (Fig. 9d).

Winds over both Lakes Erie and Ontario remained westerly with directions of 250° – 270° at the surface and 270° – 280° at 850 hPa. The surface–850 hPa layer had a lapse rate of 7.0° – $9.0^{\circ}\text{C km}^{-1}$ with an inversion present above 850 hPa from 0000 UTC 29 January to 0000 UTC 1 February as high pressure moved southeast into central Ohio (Fig. 9g). Surface winds remained westerly over Lake Erie, as 850-hPa winds backed northwesterly (Fig. 9h), favoring continued HRC development across the Buffalo region until the end of the event at 1500 UTC 1 February.

b. Ice cover and energy transfer

Ice cover notably increased over Lake Erie during the week leading up to the event (Figs. 2c,d). The largest changes in ice concentration occurred in the central and eastern basins with increases from 60% to $>90\%$ and $<10\%$ to about 90%, respectively. Areas having ice concentrations $<80\%$ the week prior to the event accounted for more than half ($15\,900\text{ km}^2$) the total surface area of the lake ($25\,655\text{ km}^2$), while on 29 January,

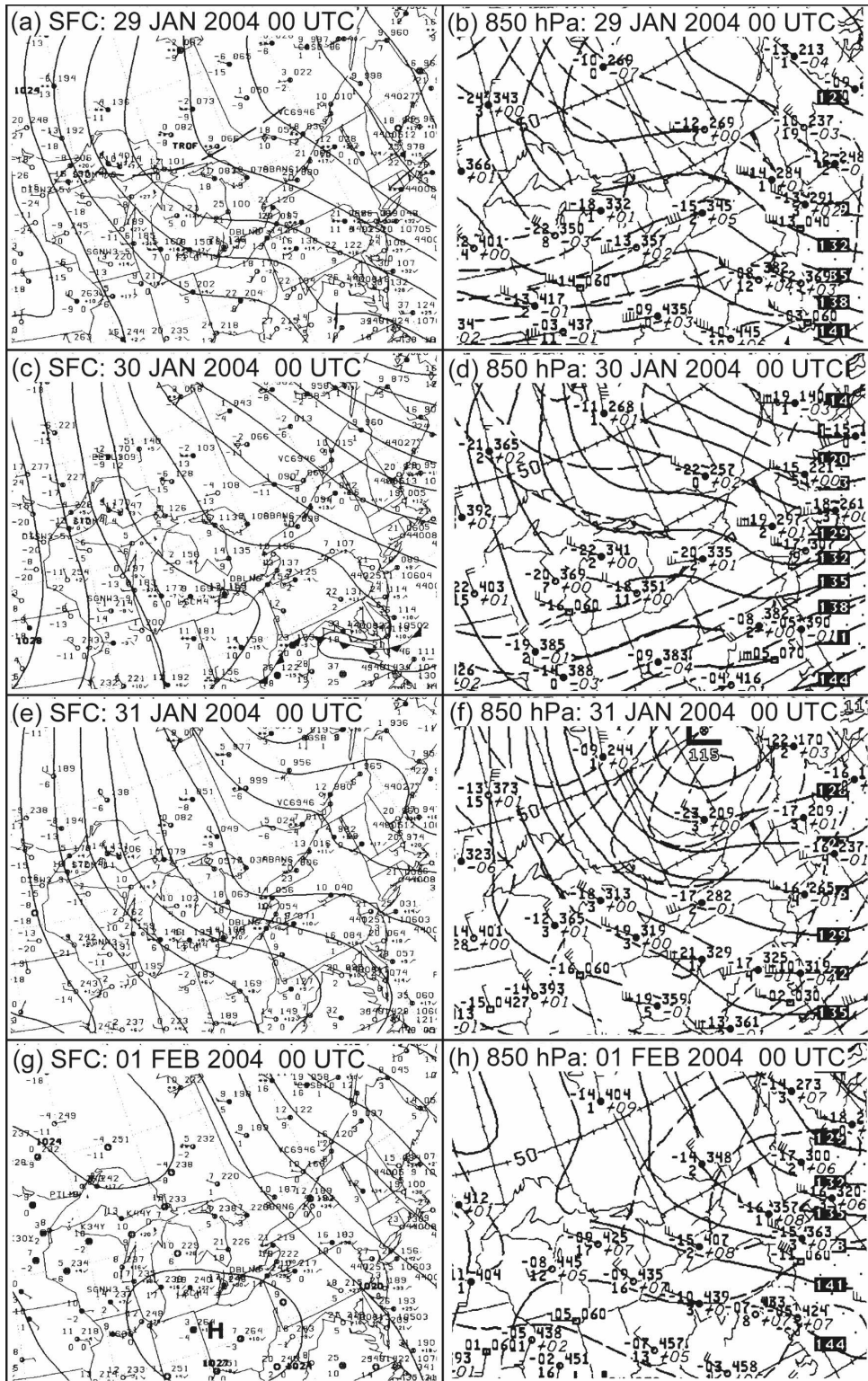


FIG. 9. Surface and 850-hPa analyses for 0000 UTC (a),(b) 29 Jan; (c),(d) 30 Jan; (e),(f) 31 Jan; and (g),(h) 1 Feb 2004. Analyses were made available from NCEP.



FIG. 10. MODIS satellite image of Lake Erie at 1615 UTC 29 Jan 2004. Darker areas represent low ice concentration or open-water regions. Image courtesy of MODIS Rapid Response Project at NASA GSFC.

during the early stages of the event, these regions were only found in the eastern basin and covered an area of 1400 km^2 (Fig. 2d). The Great Lakes ice thickness chart from the NIC for 26 January showed ice with 15–30-cm thicknesses across most of the lake, with the most substantial ice along the southern shore, and thinnest ice along the northern shore (Fig. 3b). A MODIS satellite image at 1615 UTC 29 January suggested the presence of areas of lower ice concentration in the eastern basin and along northern and western portions of the central basin (Fig. 10). The latter area was not characterized on the ice concentration chart (Fig. 2d); however, regions of 5–15-cm ice thickness (Fig. 3b) appeared to be spatially collocated with these regions present on the MODIS image.

Open-water maximum total surface heat fluxes were estimated at nearly 200 W m^{-2} during the event with sensible heat fluxes remaining about 40 W m^{-2} larger than latent heat fluxes (Fig. 11). As LE circulations and snowfall began (1500 UTC 28 January), the TET (assuming ice-free conditions) was about 3500 GW. Incorporating the 29 January 2004 ice concentration information, the Lake Erie TET decreased 95% to 175 GWatts, showing a significant impact of the ice cover

on the ability of Lake Erie to modify the stability and moisture in the lower atmosphere. Although the TET calculation is an estimate based on the ice concentrations from Fig. 2d, the aforementioned 95% reduction in energy transfer may be overestimated by as much as 10% because of errors inherent in the development of the NIC ice charts (e.g., Partington et al. 2003) and the greater area of low ice concentration observed with MODIS imagery.

c. Snowband evolution and mesoscale analysis

Two distinct time periods of continuous heavy snowfall downwind of Lake Erie occurred during the 4-day event and led to significant snowfall totals in western New York. For example, Perrysburg and Forestville, New York, had 4-day snowfall amounts of 45.7 and 48.3 cm, respectively, and East Aurora and South Wales, New York, recorded 63.5 and 58.4 cm, respectively (Fig. 1b). Two shoreline bands and three periods of HRC affected areas of western New York. Both shoreline band time periods (numbered 2 and 4) affected a collocated geographic region east of Lake Erie in southwestern New York (Fig. 12). Fetch distances in-

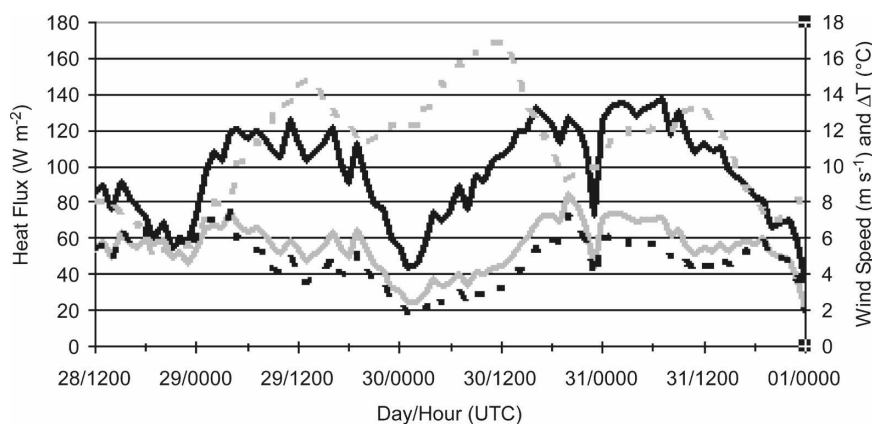


FIG. 11. Time series of lake-area-average sensible heat flux (black solid), latent heat flux (gray solid), wind speed (black dashed), and lake-air temperature difference (ΔT ; gray dashed) for Lake Erie during the 2004 event.

corporated nearly the entire length of the lake. The three periods of HRC formed during time periods of west-northwesterly winds and impacted the same region. Interestingly, the development of snowbands during this event, which resulted in greater snowfall totals than those recorded for the 12–14 February 2003 case, occurred under conditions with more extensive ice coverage on Lake Erie. Further discussion comparing the two cases is provided in section 5.

HRC LE circulations developed at 1500 UTC 28 January as synoptic precipitation exited the region to the east (period 1 in Fig. 12). At 2100 UTC 28 January radar reflectivity showed a consolidation of the HRC during a transition to westerly surface winds leading to a weak (20–25 dBZ) shoreline band by 2300 UTC 28 January downwind of regions having 9/10–10/10 ice concentration. As the wind direction shifted toward southwesterly, the band repositioned south of Buffalo by 0300 UTC 29 January and along an enhanced temperature gradient near the south Lake Erie shoreline (period 2 in Fig. 12). The surface temperature gradient increased as temperatures west and south of the lake decreased during the period and the modified air over the ice-covered lake remained at about -8°C . By 1000 UTC the shoreline band had segmented into a widespread region of west–east-oriented HRC bands that extended to the Pennsylvania border (period 3 in Fig. 12). The KDKK meteogram (Fig. 13) clearly shows the timing of the change between SB and HRC time periods was associated with wind direction changes of about 30° , the SB period having more southwesterly winds from 250° .

The extent of the HRC in the vicinity of Lake Erie is clearly visible in the MODIS satellite image at 1615 UTC 29 January (Fig. 10); however, based on the

KBUF and KCLE WSR-88D radar reflectivity at this time not all of the region with cloud cover was receiving snowfall and was spread over a larger area than the small region of 7/10–8/10 ice concentration in the eastern lake basin. This suggests that the LE clouds and precipitation were not directly linked only to the areas of low ice concentration, but their development was likely also aided by surface fluxes over higher ice concentration areas associated with low ice thicknesses, and atmospheric modification from the presence of upstream lakes. The coherent HRC slowly dissipated just after 1800 UTC 29 January with very light snowfall continuing over the Buffalo area until 0100 UTC 30 January. By 1700 UTC 30 January a coherent shoreline band developed south of Buffalo and remained steady-state in location and intensity (25–30 dBZ) until 1600 UTC 31 January (period 4 in Fig. 12). Figure 13 shows that wind, temperature, and humidity conditions at KDKK remained fairly constant during this extended period. The multiday event ended as wind directions shifted to northwesterly allowing HRC to develop east of Lake Erie with lighter LE snowfall lasting until 1500 UTC 1 February.

5. Discussion and summary

It is generally understood that extensive regions of significant lake ice-cover impact LE snow storms by decreasing the upward heat and moisture fluxes from the lake surface; however, it is only recently that studies have been conducted to more thoroughly examine this relationship (e.g., Gerbush et al. 2008). For both events presented in the current investigation, a variety of ice cover conditions and meso- and synoptic-scale factors helped support lake-effect snow storm development,

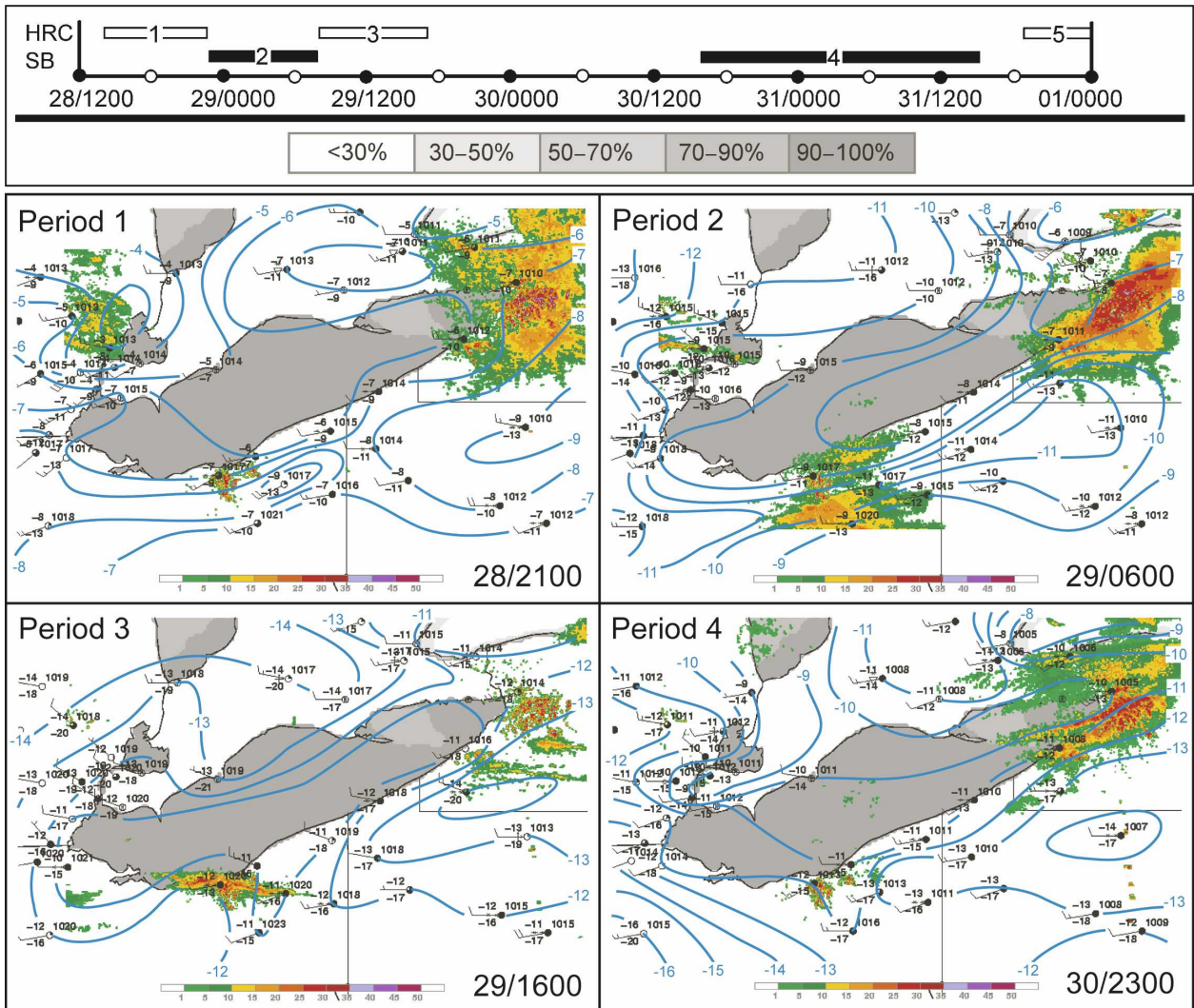


FIG. 12. As in Fig. 7, but showing summary of lake-effect type categorized as (a) SBs and (b) widespread coverage (HRC) as determined from WSR-88D reflectivity fields during the 2004 event.

lead to the transitions in LE convective type, and resulted in noteworthy snowfalls near Lake Erie.

Back-trajectory analyses for the 2003 case showed that parcels below 500 m spent a very limited percentage of fetch over areas with less than 9/10–10/10 ice concentration (Fig. 14). All LE time periods for the 12–14 February 2003 case, except periods 2 and 6 (Fig. 7), had very similar trajectories over the eastern and central basin. Time period 2 corresponded to a LE shoreline band with an upwind connection to Lake Michigan and showed a trajectory more southwesterly along the long axis of Lake Erie. The air along this trajectory interacted with ice concentrations of $\leq 8/10$ for a greater distance, although this still represented a small percentage of the fetch (i.e., 15.8%). The more extensive and coherent shoreline band during period 2

was supported by favorable upwind available moisture content, existing upwind low-level convergence, and a fetch corresponding to a longer duration of air over Lake Erie, which included lower ice concentration regions.

Lake Erie was extensively covered with 9/10–10/10 ice concentrations during the 2004 case, except for a small area of the eastern basin. This situation resulted in nearly all portions of the back trajectories positioned over only high ice concentration regions (Fig. 14c); however, the trajectory paths for both SB and HRC periods allowed for long fetch distances across the ice-covered lake (i.e., oriented close to the long axis of lake).

During both cases, there was very little opportunity for the transfer of energy to the atmosphere directly

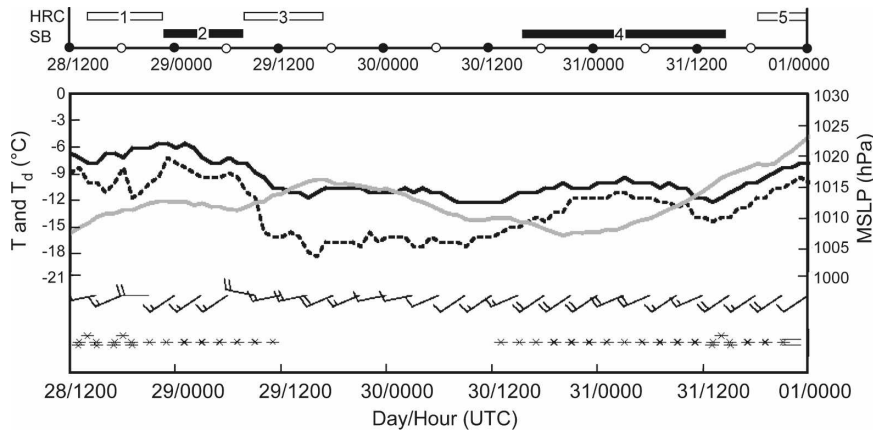


FIG. 13. Meteoagram from KDKK for 2004 event showing temperature (T : black solid), dewpoint temperature (T_d : black dashed), MSLP (gray solid), wind barbs with speed and direction information, and weather conditions. The time line of HRC and SB lake-effect precipitation periods also are shown. Winds are represented as 2.55 and 5.1 m s^{-1} for short and long barbs, respectively. Report of weather conditions uses standard NWS symbols. The location of KDKK is shown in Fig. 2a.

from open-lake waters. This was illustrated in the calculation of the TET for each case with a large reduction from the open-water values for Lake Erie. This was also the situation regardless of fetch direction or back-

trajectory path because of the extensive regions of high ice concentration and solid ice cover. A recent observational study examining ice-lake-atmosphere exchange in the Great Lakes by Gerbush et al. (2008) may

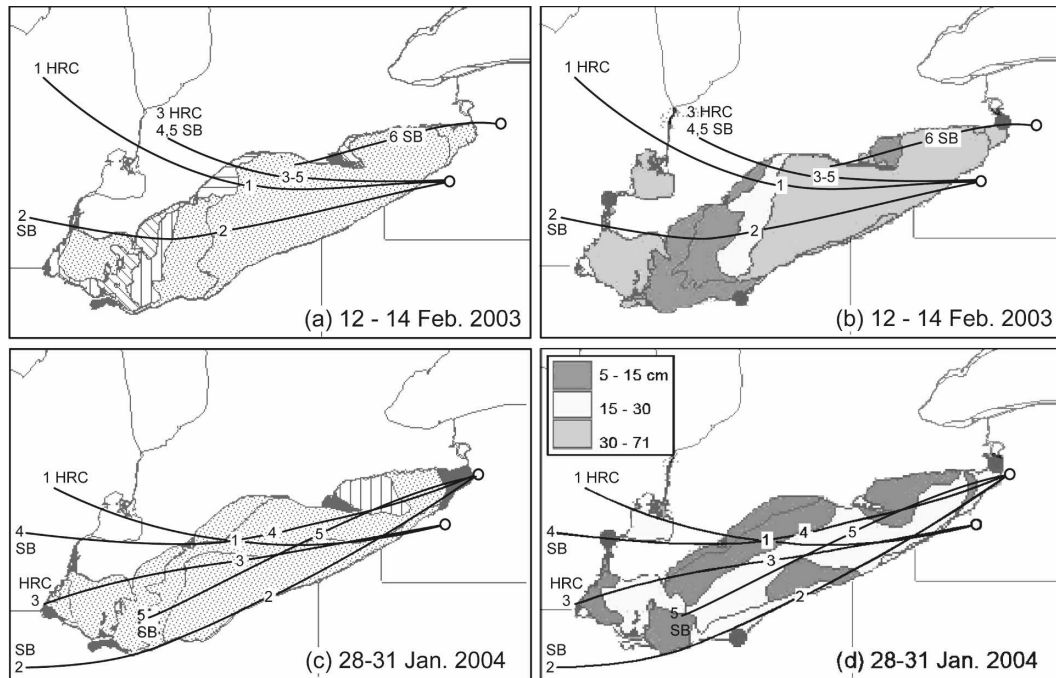


FIG. 14. Back-trajectory analyses for the Lake Erie SB and HRC time periods during the (a),(b) 2003 and (c),(d) 2004 events. (a),(c) Trajectories on ice concentration fields. (b),(d) Trajectories on ice thickness fields. The numbered labels correspond to SB and HRC time periods during each event (as in Figs. 7 and 11). Position of labels denotes the location of the parcel at 6-h intervals during the 12-h trajectory. Ice concentration is shown in (a) and (c) using the same legend as in Fig. 2.

help to provide some insight into how Lake Erie supported LE snow under the conditions described for the 2003 and 2004 cases. They reported that the relationships of latent heat flux and sensible heat flux to ice concentration can be represented by linear and nonlinear regressions, respectively. Gerbush et al. (2008) showed that latent heat flux remained at approximately 13% of the open-water value with 90% (i.e., 9/10) ice concentration regardless of forcing conditions (see their Fig. 9). More interestingly, their analyses showed that as environmental conditions provided a setting for greater sensible heat fluxes, the relationship to ice concentration became more nonlinear with the largest decrease in fluxes occurring as ice concentration increased from about 70%–100%. Gerbush et al. (2008) showed that over their range of forcing conditions the sensible heat flux at 90% ice concentration varied from about 23% to 58% of the open-water value and areas with ice concentrations <70% had sensible heat fluxes similar to open-water values (see their Fig. 7).

The evolution of the estimated sensible and latent heat fluxes for the 2003 and 2004 cases are shown in Figs. 6 and 11, respectively. The average sensible and latent heat fluxes for the case study time period during 2003 (2004) were 95.3 W m^{-2} (96.9 W m^{-2}) and 57.9 W m^{-2} (54.8 W m^{-2}), respectively. The results from Gerbush et al. (2008) suggest that for our cases when the lake was extensively covered by 90% ice concentration, the average sensible heat fluxes were reduced to approximately 56 W m^{-2} and the latent heat fluxes decreased to nearly 7 W m^{-2} . These values are relatively low when compared to winter surface heat fluxes reported for open-water regions of the Great Lakes during LE conditions (e.g., Kristovich and Laird 1998; Laird and Kristovich 2002). However, the reduction of the open-water fluxes using the information provided by Gerbush et al. (2008) may result in an underestimate of the sensible heat fluxes since the LE forcing conditions during the 2003 and 2004 cases were significantly greater than existed during the case examined by Gerbush et al. (2008). The ability of the 2003 and 2004 cases to produce noteworthy LE snow storms over an extensively ice-covered lake demonstrates that the relationship between surface heat fluxes and ice concentration needs to be examined in a more inclusive range of LE conditions. These cases also provide examples showing that the development of lake-effect precipitation bands over extensively ice-covered lakes need not be directly linked to fractures or areas of low concentration in the ice field.

An important difference between the 2003 and 2004 cases was the distribution of ice thickness for Lake Erie

(Figs. 3 and 14b,d). Nearly 63% of the surface area of Lake Erie was covered by ice having a thickness of ≥ 30 cm during the 2003 event; while thinner ice existed during the 2004 event with similar-sized areas of the lake having ice thickness between 15 and 30 cm (56% of lake area) and ≤ 15 cm (44% of lake area). Because the event-average sensible and latent heat fluxes were similar during the two cases, we can use a simplified equation of heat conduction through ice as a first-order estimate to examine the impact that differences in ice thickness across the 2003 and 2004 cases had on resulting sensible heat fluxes. Heat conduction (HC) through ice from the bottom to the surface can be expressed as

$$\text{HC} = \kappa \frac{T_b - T_s}{I_z}, \quad (1)$$

where κ is the heat conduction coefficient ($=2.03 \text{ W K}^{-1} \text{ m}^{-2}$), T_b is the temperature at the bottom of the ice (i.e., lake water temperature), T_s is the temperature at the top of the ice, and I_z is the ice thickness. Analyses of the ice thickness distributions shown in Figs. 3 and 14 b,d indicate that during the 2003 event 63%, 11%, and 25% of Lake Erie was covered with ice thicknesses in the range of 30–71, 15–30, and 5–15 cm, respectively. During the 2004 event, 0%, 56%, and 44% of Lake Erie was covered with ice thicknesses in the range of 30–71, 15–30, and 5–15 cm, respectively. Calculations using data along with Eq. (1) suggest that the thicker ice on Lake Erie during the 2003 event caused an additional reduction in the sensible heat flux of 42.5% when compared to the already restricted fluxes resulting from thinner ice cover conditions during the 2004 event. These analyses suggest that weather prediction models should not only include information regarding ice concentration distribution, but should consider incorporating information on the distribution of ice thickness.

General meteorological intuition suggests that the development of LE snow storms is inhibited when lakes are extensively ice covered. The two cases presented in this article provide the first examination of Great Lakes lake-effect snow storms that developed in association with an extensively ice-covered lake. During both events the collocation of LE SBs and HRC regions downwind of Lake Erie was responsible for the noteworthy accumulated snowfall totals. The thinner ice cover along with the more favorable fetch directions during the 2004 event likely aided the development of the more intense SB time periods and the resulting greater snowfall in areas southeast of Lake Erie. Although Lake Erie had regions with lower ice concentration during the 2003 event, thicker ice cover was present across a greater area of the lake and most tra-

jectories during the LE time periods were positioned over higher ice concentration regions. In addition, the 2003 LE snowbands during both SB and HRC time periods had a shorter duration and impacted the same region to a lesser degree than the 2004 case. These combined factors likely contributed to the lower snowfall totals across southwestern New York during the 2003 event.

Acknowledgments. The first author conducted a major portion of this research during the 2005 summer undergraduate research program at Hobart and William Smith (HWS) Colleges. We appreciate the thoughtful input and reviews of this manuscript provided by David Kristovich of the Illinois State Water Survey and two anonymous reviewers. We thank both David Zaff and Thomas Niziol of the NWSFO at Buffalo for their assistance in providing snowfall data and archived forecast summaries. The authors gratefully acknowledge the NOAA/Air Resources Laboratory (ARL) for the provision of the HYSPLIT transport and dispersion model and/or READY Web site (<http://www.arl.noaa.gov/ready.html>) used in this publication. This research was supported by the National Science Foundation under Grant ATM-0512233. Additional support was provided by the Office of the Provost at HWS. Any opinions, findings, conclusions, and recommendations expressed in this publication are those of the authors and do not necessarily reflect the views of the National Science Foundation.

REFERENCES

- Assel, R. A., 1990: An ice-cover climatology for Lake Erie and Lake Superior for the winter seasons 1897–98 to 1982–83. *Int. J. Climatol.*, **10**, 731–748.
- , 1999: Great Lakes ice cover. *Potential Climate Change Effects on Great Lakes Hydrodynamics and Water Quality*, D. C. L. Lam and W. M. Schertzer, Eds., American Society of Civil Engineers, 1–21.
- , D. C. Norton, and K. C. Cronk, 2002: A Great Lakes ice cover digital data set for winters 1973–2000. NOAA Tech. Memo. GLERL-121, Great Lakes Environmental Research Laboratory, Ann Arbor, MI, 46 pp.
- Baker, D. G., 1976: The mesoscale temperature and dew point fields of a very cold airflow across the Great Lakes. *Mon. Wea. Rev.*, **104**, 860–867.
- Ballentine, R. J., A. J. Stamm, E. E. Chermack, G. P. Byrd, and D. Schleede, 1998: Mesoscale model simulation of the 4–5 January 1995 lake-effect snowstorm. *Wea. Forecasting*, **13**, 893–920.
- Braham, R. R., Jr., 1983: The Midwest snowstorm of 8–11 December 1977. *Mon. Wea. Rev.*, **111**, 253–272.
- Draxler, R. R., and G. D. Hess, 1998: An overview of the Hysplit_4 modeling system for trajectories, dispersion, and deposition. *Aust. Meteor. Mag.*, **47**, 295–308.
- , and G. D. Hess, 1997: Description of the Hysplit_4 modeling system. NOAA Tech. Memo. ERL ARL-224, December, 24 pp.
- , and G. D. Rolph, cited 2003: HYSPLIT (HYbrid Single-Particle Lagrangian Integrated Trajectory) Model. NOAA/Air Resources Laboratory. [Available online at <http://www.arl.noaa.gov/ready/hysplit4.html>.]
- Fetterer, F., and C. Fowler, 2006: National Ice Center Arctic sea ice charts and climatologies in gridded format. National Snow and Ice Data Center, Boulder, CO, digital media. [Available online at http://nsidc.org/data/docs/noaa/g02172_nic_charts_climo_grid/index.html.]
- Garratt, J. R., 1992: *The Atmospheric Boundary Layer*. Cambridge University Press, 316 pp.
- Gerbush, M. R., D. A. R. Kristovich, and N. F. Laird, 2008: Mesoscale boundary layer and heat fluxes variations over pack ice-covered Lake Erie. *J. Appl. Meteor. Climatol.*, **47**, 668–682.
- Jeffries, M. O., and K. Morris, 2006: Instantaneous daytime conductive heat flow through snow on lake ice in Alaska. *Hydrol. Process.*, **20**, 803–815.
- Kristovich, D. A. R., and N. F. Laird, 1998: Observations of widespread lake effect cloudiness: Influences of lake surface temperature and upwind conditions. *Wea. Forecasting*, **13**, 811–821.
- , and M. L. Spinar, 2005: Diurnal variations in lake-effect precipitation near the western Great Lakes. *J. Hydrometeorol.*, **6**, 210–218.
- , and Coauthors, 2000: The Lake-Induced Convection Experiment and the Snowband Dynamics Project. *Bull. Amer. Meteor. Soc.*, **81**, 519–542.
- Laird, N. F., and D. A. R. Kristovich, 2002: Variations of sensible and latent heat fluxes from a Great Lakes buoy and associated synoptic weather patterns. *J. Hydrometeorol.*, **3**, 3–12.
- , and —, 2004: Comparison of observations with idealized model results for a method to resolve winter lake-effect mesoscale morphology. *Mon. Wea. Rev.*, **132**, 1093–1103.
- Lytle, V. I., and S. F. Ackley, 1996: Heat flux through sea ice in the western Weddell Sea: Convective and conductive transfer processes. *J. Geophys. Res.*, **101** (C4), 8853–8868.
- Maykut, G. A., 1978: Energy exchange over young sea ice in the central Arctic. *J. Geophys. Res.*, **83** (C7), 3646–3658.
- Niziol, T. A., W. R. Snyder, and J. S. Waldstreicher, 1995: Winter weather forecasting throughout the eastern United States. Part IV: Lake effect snow. *Wea. Forecasting*, **10**, 61–77.
- Partington, K., T. Flynn, D. Lamb, C. Bertoia, and K. Dedrick, 2003: Late twentieth century Northern Hemisphere sea-ice record from U.S. National Ice Center ice charts. *J. Geophys. Res.*, **108**, 3343, doi:10.1029/2002JC001623.
- Rauber, R. M., and F. M. Ralph, 2004: An implementation plan for cool season quantitative precipitation forecasting. United States Weather Research Program, 54 pp. [Available online at <http://box.mmm.ucar.edu/uswrp/implementation/CSQPF.pdf>.]
- Reinking, R. F., and Coauthors, 1993: The Lake Ontario Winter Storms (LOWS) project. *Bull. Amer. Meteor. Soc.*, **74**, 1828–1849.
- Richards, T. L., 1964: The meteorological aspects of ice cover on the Great Lakes. *Mon. Wea. Rev.*, **92**, 297–302.
- Rodriguez, Y., D. A. R. Kristovich, and M. R. Hjelmfelt, 2007: Lake-to-lake cloud bands: Frequencies and locations. *Mon. Wea. Rev.*, **135**, 4202–4213.

- Rolph, G. D., cited 2003: Real-time Environmental Applications and Display System (READY). NOAA/Air Resources Laboratory. [Available online at <http://www.arl.noaa.gov/ready/hysplit4.html>.]
- Rose, B. L., 2000: The role of upstream lakes in determining downstream severe lake-effect snowstorms. Ph.D. dissertation, University of Illinois, 183 pp. [Available from ProQuest Information and Learning, P. O. Box 1346, Ann Arbor, MI 48106.]
- Sturm, M., D. K. Perovich, and J. Holmgren, 2002: Thermal conductivity and heat transfer through snow on the ice of the Beaufort Sea. *J. Geophys. Res.*, **107**, 8043, doi:10.1029/2000JC000409.
- Zulauf, M. A., and S. K. Krueger, 2003: Two-dimensional cloud-resolving modeling of the atmospheric effects of Arctic leads based upon midwinter conditions at the Surface Heat Budget of the Arctic Ocean ice camp. *J. Geophys. Res.*, **108**, 4312, doi:10.1029/2002JD002643.